Magnetic Signature-Based Model Using Machine Learning for Electrical and Mechanical Faults Classification of Wind Turbine Drive Trains

Akhyurna Swain, Elmouatamid Abdellatif, Philip W.T. Pong

Magnetic Signature-Based Model Using Machine Learning for Electrical and Mechanical Faults Classification of Wind Turbine Drive Trains

Akhyurna Swain,
Elmouatamid Abdellatif
Philip W.T. Pong
Department of Electrical and Computer Engineering,
New Jersey Institute of Technology
NJ 07102, USA

Abstract—Signal processing and fault indicators analysis are essential for efficient fault detection, classification, and diagnosis of wind turbines. Accordingly, existing works proposed the installation of multiple intrusive sensors (e.g., current, voltage, frequency) for data collection in order to detect and classify the faults in wind turbine drive train (WTDT). However, these sensors are scattered on the drive train and have a limited local reach on its components making it technically difficult to install. Therefore, signals from these sensors are not able to detect multi parameter phenomena such as coupling of the mechanical and electrical components of the drive train which contains essential fault information. This work proposes the use of magnetic signatures as fault condition indicators of the complete drive train due to the ability of contactless measurement of this signal without opening the main components of the drive train. This is achieved by performing non-destructive magnetic modeling and analysis of the entire drive train. The air gap magnetic flux density of the wind generator is demonstrated as a good fault condition indicator for different common faults occurring on the gearbox, bearings, and the generator. The proposed model is validated using a supervised machine learning classification algorithm in a way to distinguish between electrical and mechanical faults.

***Index Terms*—Condition Monitoring Systems, Fault indicators, Magnetic modeling, Magnetic Signature, Wind turbine drivetrains.**

I. INTRODUCTION

Rapid deployment of wind energy is essential to meet the federal and state goals for sustainable energy development. However, investments in wind energy hugely depend on the competitive electricity prices of various energy sources including maintenance cost, fault detection, and restoration of damaged components [1]. Therefore, there is an urgent need to reduce the cost of wind technologies to make them viable for long term investments. Currently, the monitoring and maintenance paradigm in wind turbines is shifting from a reactive, periodic and usage based maintenance to a predictive, regular and condition based maintenance [4]. This requires continuous monitoring and fault prognosis of various components. Typical data sources considered for condition monitoring in wind turbine drive trains are based on supervisory control and data acquisition (SCADA) data (e.g., current, voltage, frequency), vibration monitoring, acoustics monitoring, temperature monitoring, and current signature analysis. However, there are certain disadvantages to these existing monitoring techniques. Most of these techniques except acoustic monitoring requires intrusive sensors [5]. The invasiveness of these sensors makes them difficult for installation. Further, these installations can cause structural abrasions and interfere with the flow of current in certain components, increasing their remaining useful life. Thus, they add an extra cost during replacement and upgrading of components and the monitoring is restricted only to certain individual components. Therefore, mechanical and electrical faults have the same effects on these measurements making the classification of faults a complicated task and requiring the use of additional sensing such as the magnetic field variable. Therefore, data on dynamic and interdependent variables of the wind turbines are generally not available from these sensors data.

Wind turbine drive trains are most vulnerable to faults due to the presence of dynamic components (e.g., electrical, mechanical) that are coupled to each other and hence its downtime poses a huge impact on the cost-effectiveness of the installation [6]. Further, the presence of electromagnetic coupling among its components generates dynamic parameters (e.g., magnetic signature, electromagnetic torque) that can be considered fault signatures. However, they are neglected during individual component sensing. Therefore, current literatures have acknowledged the need for efficient modeling of drive trains to capture these dynamic parameters [7]. This paper proposes to employ magnetic modeling of drive trains to obtain dynamic

parameters that are a result of electromagnetic coupling among its components and evaluate them as condition indicators for fault detections. The magnetic signature is proposed as a fault condition indicator for condition monitoring of the WTDT. Various mechanical and electrical faults are simulated on the permanent magnet synchronous generator (PMSG) gearbox and the bearing of WTDT, while K-nearest neighbors (KNN) supervised machine learning model is used for faults classification. This method of using magnetic signatures as fault condition indicators is unique in literature and provides a novel non-destructive condition monitoring system (CMS) approach for the entire WTDT.

The remainder of this paper is organized as follows: Section 2 investigates the main common fault indicators in wind turbine drive train. Section 3 explores the modeling of the used WTDT with the magnetic equivalent circuit of PMSG coupled with gearbox. The faults tested and introduced on wind turbine drive train are presented in Section 4 with the main parameters used for the simulation in JMAG and Solidworks. Results and discussion are presented in Section 5 to show the usefulness of the proposed method to classify mechanical and electrical faults. Conclusions and perspectives are discussed in Section 6.

II. Common Fault Indicators in Wind Turbines Drive Train Used for Condition Monitoring System

SCADA data offers a good selection of system parameters for condition monitoring of wind turbines [8]. In general, data is recorded at 10-minute averages of 1Hz sampled values along with its maximum, minimum and standard deviations. The range of data collected includes environmental variables such as wind speed, wind direction and electrical variables such as generator voltages, phase currents, frequencies, along with temperature variables and other control variables (e.g., pitch angle, yaw angle). However, in order to model continuous fault monitoring systems, SCADA datasets should be available for a long period of time, typically over years. Availability of such data is scarce. Further, the collected SCADA data is only valid for the same wind turbine manufacture due to the non-existence of unique standards of data collection in the wind turbines. Vibration based condition monitoring [5] is another type of commercially available CMS [5]. It involves evaluating fault development in machines operating in 10–200 Hz frequency range. Hence, accelerometers are restricted to the low frequency range. Vibration signals, especially from the gearbox, suffer from complications due to nonlinearity and nonstationary nature of signals. Finally, vibration signals are disposed to contamination by environmental noise. Recently, acoustic emissions [9] have been a topic of interest [9]. However, deployment of infrared camera makes the CMS expensive and adds to the investment cost. Temperature based CMS [10] have been used to monitor multiple components of the wind turbine such as generator windings, bearings and oil [10]. Mainly, the temperature sensors provide local rise in temperature due to their embedded nature. This local information limits the measurement data and hot spots developed over a larger area and measurement of temperature gradient, especially in fluids becomes difficult. Although thermal imaging could be applied to benefit the issue, infrared cameras would again add to the investment cost. Finally, electrical signals such as voltage or current signals [5] measured from the wind generator have been employed in CMS [5]. Nonetheless, these signals have a low signal-to-noise ratio due to modulation of fundamental frequency of signal with other harmonic components. Further, the fault signals here have nonstationary signatures due to the intermittent nature of wind and nonstationary operation of wind turbines. Finally, magnetic flux monitoring has been employed to detect inter-turn short circuit faults in doubly fed induction generators. Consequently, magnetic signatures have not been employed for CMS. Magnetic signatures of wind generators are privileged for fault indicators since magnetic sensors are non-intrusive in nature. This paper employs magnetic signatures as fault condition indicators and investigates their ability to aid with the CM of the entire wind turbine drive train.

III. Magnetic Modeling of Wind Turbine Drive Trains

Typical wind turbine drive trains consist mechanical components such as gearbox, bearings, rotating shafts, and electrical components such as the wind generator. It has been established that these components are electromagnetically coupled with each other through a common magnetic flux which emanates from the wind generator [11]. Magnetic equivalent circuit of a PMSG is shown in fig. 1 as it is investigated in [12].

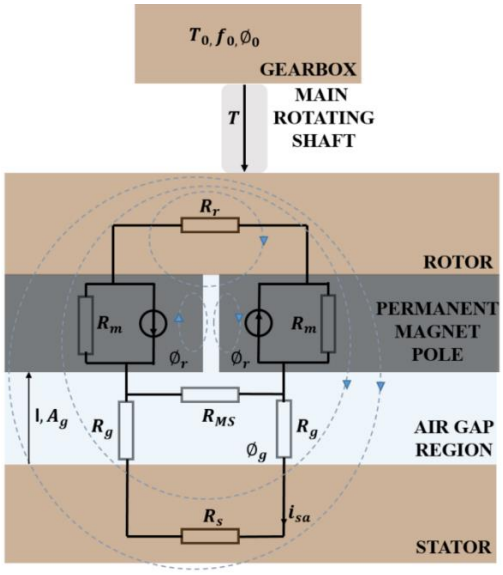

Fig 1. Magnetic Equivalent Circuit of PMSG coupled with a gearbox

From fig. 1, the air gap flux of a PMSG can be calculated in form of air gap region parameters such as the air gap length l and surface area A_g as follows (equation 1).

$$\Phi_g = 4\Phi_r R_m R_1 \Big/ \left[{}^{[2R_1 R_{MS}}\!/_{\mu_0 A_g} + (R_r + 2R_m)\left(\frac{2l}{\mu_0 A_g} + R_s + R_1\right)\right] \quad (1)$$

Further, due to the nature of electromagnetic coupling, the fluctuations in the characteristic parameters of these components will alter the common magnetic flux distribution on the wind generator. This change is reflected in the input torque and output current produced by the wind generator as described in the following equations (2, 3, 4). The Mechanical torque T links the electromagnetic and mechanical characteristics of the gearbox with the PMSG and can be expressed as follows [11].

$$T = T_{avg} + T_0 \cos(2\pi f_0 t + \phi_0) \quad (2)$$

where T_{avg} is the average value of torque while T_0, f_0, ϕ_0 are the characteristic amplitude, frequency and phase of the oscillatory components induced by the vibrations in the gearbox. This torque T of a PMSG can also be expressed in terms of stator phase current i_{sa} as follows.

$$T = -\frac{3}{2}\rho M i_{sa} i_f \sin\delta_i \quad (3)$$

Further, the stator phase current of a synchronous machine can be expressed as follows.

$$i_{sa} = i_{s0}\sin(2\pi f_s t + \phi_g) + \frac{1}{2}A_s\{\cos[2\pi(f_s - f_0)t - \phi_g]\} + \cos[2\pi(f_s + f_0)t + \phi_g] \quad (4)$$

where $f_s \pm f_0$ are the characteristic fault frequencies. Hence, the air-gap flux ϕ_g of a PMSG is proportional to stator current i_{sa} and the electromagnetic torque T. Therefore, the characteristic fault frequencies f_0 induced due to vibrations in the gearbox can be expected to be reflected in the air gap flux ϕ_g of the wind turbine. Hence through this process of magnetic modeling, the air gap flux can be utilized as a fault condition indicator to detect fault frequencies on the gearbox as well as the PMSG, thus accounting for complete CMS of the entire wind turbine drive train.

IV. Magnetic Fault Indicators of Wind Turbine Drive Trains

In order to obtain various magnetic fault indicators for CMS of the WTDT, the magnetic modeling of a PMSG coupled to a gearbox through a rotating shaft is realized. This is conducted by performing finite element analysis (FEA) of the wind turbine drive train through the process of co-simulation. The two co-simulation software used are JMAG for the modeling of PMSG and Solidworks for the modeling of the gearbox with bearings and the rotating shaft [13]. The drive train is designed with a 400V, 60Hz, 24 slots and 4 pole PMSG coupled to a planetary gearbox consisting of 5 gears with a pre-defined gear ration of 0.166. Details of the model parameters have been tabulated in Table I. Next, through mesh generation and FEA of the entire wind turbine drive, magnetic signatures of the PMSG such as the air gap magnetic flux density data is collected. Finally, various faults are introduced in both the electrical component as well as the mechanical component as shown in Table II.

Additionally, through FEA, the air gap magnetic flux density data is collected for each fault case. These faulty data is compared in order to identify the accurateness of these parameters as fault condition indicators.

TABLE I. Wind Turbine Drive Train Model Parameters

Component	Values
Rated Voltage of PMSG(V)	400
Frequency of PMSG (Hz)	60
Number of Slots/Poles of PMSG	24/4
Type of gearbox	Planetary
Number of gears	5
Gear Ratio	1.66
Speed of gearbox rpm (Input, Output)	16,100

TABLE II. List of faults introduced on wind turbine drive train

Category	Component	Type of Fault
Mechanical	Gearbox	Broken tooth
	Bearings	Inner race fault
Electrical	Permanent Magnet	Demagnetization
	Rotor	Eccentricity

V. Results and Discussion

First through FEA, the magnetic modeling of the wind turbine drive train is realized. Fig. 2 presents the magnetic flux density distribution that was generated through the magnetic transient analysis of the PMSG.

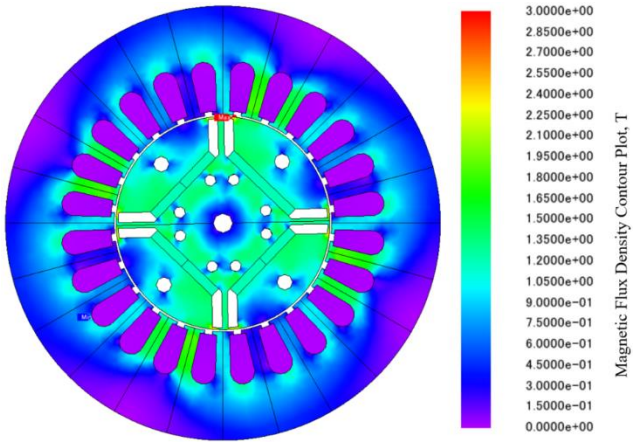

Fig. 2. Magnetic flux density distribution on surface of PMSG through magnetic modeling of wind turbine drive train

This is considered as a normal operating case of the driver's train. Consequently, in order to verify the presence of electromagnetic coupling among the PMSG and the gearbox, a fault was introduced on the gear as a broken tooth. Then magnetic transient analysis of this drive train model with the broken gear tooth was analyzed through FEA. The air gap magnetic flux density due to the broken gear tooth was obtained and compared with the air gap magnetic flux density obtained in the first step. A comparison graph is presented in Fig. 3.

Fig. 3 shows a decrease in the amplitude of the air gap magnetic flux density when broken gear tooth fault is introduced. This is due to the broken tooth would cause vibrations on the gear resulting in non-uniform angular velocity on the rotating shaft. This would change the speed

of the shaft which in turn would change the rotor speed and distribution of the stator current on the PMSG, in that way changing the magnitude and distribution of its magnetic flux density.

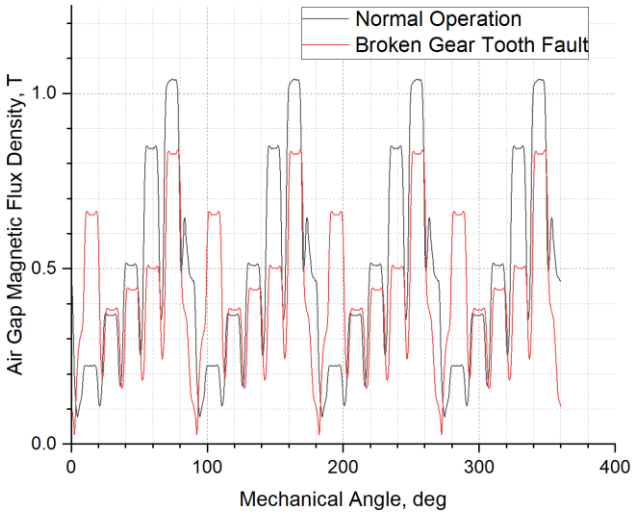

Fig. 3. A comparative analysis of air gap magnetic flux density of the PMSG for normal operation vs broken gear tooth fault of the drive train

By comparing the curves in Fig. 3, the presence of electromagnetic coupling between the PMSG and the gearbox can be verified. Further, due to this electromagnetic coupling, the change of the gearbox's parameters is reflected in the magnetic flux density of the PMSG. In addition, the faults in various components according to Table II are introduced and magnetic modeling for FEA analysis of the drive train is conducted. The air gap magnetic flux density of all fault cases is plotted and compared with the normal operating case (Fig. 4).

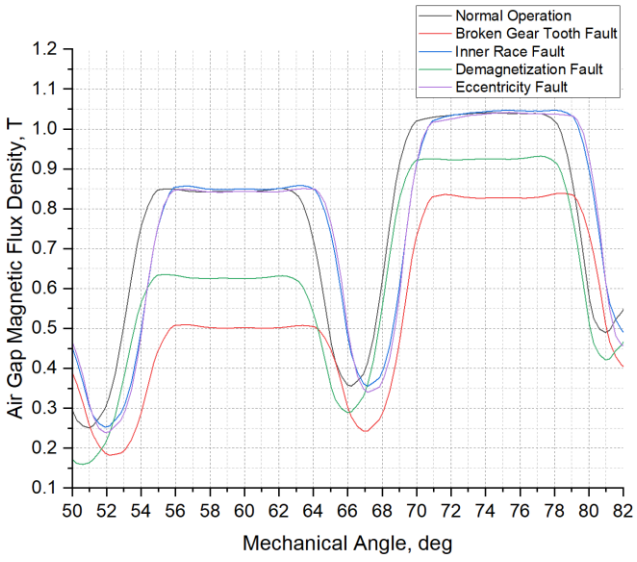

Fig. 4. A comparative analysis of air gap magnetic flux density of the PMSG for normal operation vs various faults cases on the drive train

The comparative analysis in Fig. 4 clearly shows different values of amplitude of the air gap magnetic flux density for various faults introduced on different components of the drive train. From this figure, it is clearly observed that the faults on mechanical and electrical components have much lower amplitude than the normal operation case. Therefore, it is shown that the air gap magnetic flux density is a good fault indicator for the studied faults.

Moreover, in order to show the efficiency of the air gap magnetic fault density as a good fault condition indicator for fault classification in CMS, a machine learning based model was designed for single class classification. Here the broken gear tooth fault signal is chosen to be classified from the normal operation. The air gap magnetic flux density of the signal is first analyzed under frequency domain signal processing and time-frequency domain signal processing. For the frequency domain signal processing, Fast Fourier Transform (FFT) was employed to extract the fault frequency components from the broken gear tooth signal. This was then compared with the FFT of signal under normal operation to extract fault condition indicators as shown in Fig. 5. For the time-frequency domain signal processing, Hilbert transform (HT) was employed to extract the analytical signals. Fault features corresponding to Hilbert coefficients are from the broken gear tooth signal. This was then compared with the Hilbert coefficients of signal under normal operation to extract fault condition indicators as shown in Fig. 6.

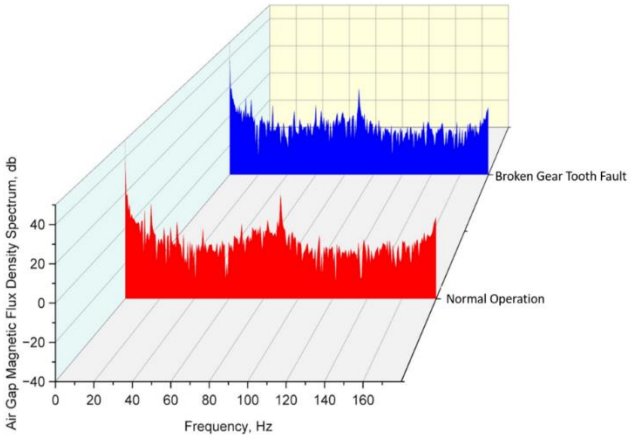

Fig. 5. A comparative FFT analysis of air gap magnetic flux density of the PMSG for normal operation vs broken gear tooth fault

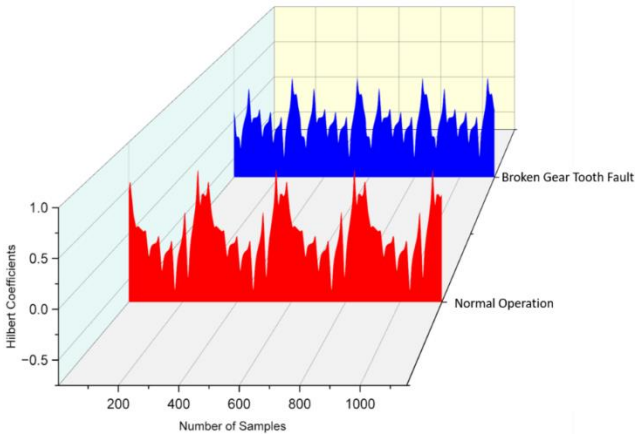

Fig. 6. A comparative HT analysis of air gap magnetic flux density of the PMSG for normal operation vs broken gear tooth faults

Following the successful signal processing, the fault indicators were fed as input model parameters to a supervised machine learning algorithm (KNN). The hyper parameters chosen for the KNN machine learning algorithm have been tabulated in Table III. Further, the classification accuracy of the two signal processing cases has been tabulated in Table IV.

TABLE III. HYPER PARAMETERS FOR ML CLASSIFICATION MODEL

Model Hyper parameters	Values
Algorithm	k-nearest neighbor
Type	Supervised
Number of neighbors	3
Distance metric	Euclidean
Distance weight	Equal

TABLE IV. CLASSIFICATION ACCURACY TABLE

Data Processing Domain	Data Processing Technique	Accuracy
Frequency Domain	FFT	0.844
Time-Frequency Domain	HT	0.781

From Table IV, it is observed that the accuracy of classification for FFT based signal processing yields better results than the HT based signal processing. This is due to the mono components of the HT coefficients that are not presented with good fault condition indicators. This can be rectified by using an adaptive filter or empirical mode decomposition to obtain intrinsic mode functions prior to obtaining the HT coefficients [14]. Further, it is acknowledged that the classification accuracy is less important than the classification accuracy of CMS conducted with other data sources such as SCADA data and vibration data [5, 9],[9] . Therefore, the paper identifies the need of working on other signal processing techniques such as statistical time domain analysis and wavelet analysis to further improve the classification accuracy.

VI. CONCLUSIONS AND PERSPECTIVES

The work investigated the use of a magnetic signature-based model for electrical and mechanical faults classification of WTDT. It was conducted by proposing the magnetic modeling of the drive train and extracting magnetic signatures that have faulty information of both the mechanical and the electrical component of the drive train. This manner of non-destructive magnetic evaluations for fault detections on the entire drive train is unique in literature and opens a new avenue of CMS. In order to improve the classification accuracy, other signal processing techniques such as statistical time domain analysis and wavelet analysis will be conducted in the future work. Finally, there is a need for a multi-class classification algorithm that can be designed to employ all the fault signals presented in Fig. 4 for fault classification of the entire wind turbine drive train.

VI. ACKNOWLEDMENT

We would like to acknowledge the funding support from the New Jersey Economic Development Authority (Award # 00089196-NJOWTRI).

REFERENCES

[1] M. Papapetrou and G. Kosmadakis, "Chapter 9 - Resource, environmental, and economic aspects of SGHE," in Salinity Gradient Heat Engines, A. Tamburini, A. Cipollina, and G. Micale Eds.: Woodhead Publishing, 2022, pp. 319-353.

[2] C. Dao, B. Kazemtabrizi, and C. Crabtree, "Wind turbine reliability data review and impacts on levelised cost of energy," Wind Energy, vol. 22, no. 12, pp. 1848-1871, 2019.

[3] T. Stehly, and Duffy, Patrick. , "Cost of Wind Energy Review. United States," 2021.

[4] A. R. Nejad et al., "Wind turbine drivetrains: state-of-the-art technologies and future development trends," Wind Energy Science, vol. 7, no. 1, pp. 387-411, 2022.

[5] W. Qiao and L. Qu, "Prognostic condition monitoring for wind turbine drivetrains via generator current analysis," Chinese Journal of Electrical Engineering, vol. 4, no. 3, pp. 80-89, 2018, doi: 10.23919/CJEE.2018.8471293.

[6] D. van Binsbergen, S. Wang, and A. R. Nejad, "Effects of induction and wake steering control on power and drivetrain responses for 10 MW floating wind turbines in a wind farm," Journal of Physics: Conference Series, vol. 1618, p. 022044, 09/01 2020, doi: 10.1088/1742-6596/1618/2/022044.

[7] S. Struggl, V. Berbyuk, and H. Johansson, "Review on wind turbines with focus on drive train system dynamics," Wind Energy, vol. 18, 02/01 2014, doi: 10.1002/we.1721.

[8] J. Tautz-Weinert and S. J. Watson, "Using SCADA data for wind turbine condition monitoring–a review," IET Renewable Power Generation, vol. 11, no. 4, pp. 382-394, 2017.

[9] A. Romero, S. Soua, T.-H. Gan, and B. Wang, "Condition monitoring of a wind turbine drive train based on its power dependant vibrations," Renewable Energy, vol. 123, pp. 817-827, 2018/08/01/ 2018, doi: https://doi.org/10.1016/j.renene.2017.07.086.

[10] O. Tonks and Q. Wang, "The detection of wind turbine shaft misalignment using temperature monitoring," CIRP Journal of Manufacturing Science and Technology, vol. 17, pp. 71-79, 2017/05/01/ 2017, doi: https://doi.org/10.1016/j.cirpj.2016.05.001.

[11] L. Q. F. Cheng, W. Qiao, C. Wei and L. Hao, "Fault Diagnosis of Wind Turbine Gearboxes Based on DFIG Stator Current Envelope Analysis," IEEE Transactions on Sustainable Energy, vol. 10, no. 3, pp. 1044-1053, July 2019, doi: 10.1109/TSTE.2018.2859764., 2019.

[12] Q. Xu, X. Liu, W. Miao, P. W. T. Pong, and C. Liu, "Online Detecting Magnet Defect Fault in PMSG With Magnetic Sensing," IEEE Transactions on Transportation Electrification, vol. 7, no. 4, pp. 2775-2786, 2021, doi: 10.1109/TTE.2021.3073630.

[13] C. L. Akhyurna Swain, and Philip W.T. Pong, "Modeling of Wind Turbine Drive Trains for Finite Element Analysis through Co-Simulation," presented at the unpublished, presented at IEEE international magnetics conference INTERMAG 2023, Sendai, Japan on May 2023., 2023.

[14] P. Konar and P. Chattopadhyay, "Multi-class fault diagnosis of induction motor using Hilbert and Wavelet Transform," Applied Soft Computing, vol. 30, pp. 341-352, 2015/05/01/ 2015, doi: https://doi.org/10.1016/j.asoc.2014.11.062.